



A deceleration model for bicycle peloton dynamics and group sorting



Hugh Trenchard^{a,*}, Erick Ratamero^b, Ashlin Richardson^c, Matjaž Perc^d

^a 805 647 Michigan Street, Victoria, BC V8V 1S9, Canada

^b University of Warwick, MOAC DTC – Senate House, Gibbet Hill Road, CV4 7AL Coventry, UK

^c University of Victoria, Department of Computer Science, PO Box 1700, STN CSC, Victoria, BC V8W 2Y2, Canada

^d Faculty of Natural Sciences and Mathematics, University of Maribor, Slovenia & Faculty of Science, King Abdulaziz University, Jeddah, Saudi Arabia

ARTICLE INFO

Keywords:

Peloton
Cycling
Sustainable output
Group sorting
Collective motion
Flocking

ABSTRACT

Extending earlier computer models of bicycle peloton dynamics, we add a deceleration parameter by which deceleration magnitude varies as a function of cyclist strength. This model is validated by applying speed data from a mass-start race composed of 14 cyclists, and running simulation trials using 14 simulated cyclists that generated positional profiles which compare well with the positional profiles observed in the actual mass-start race data. Keeping constant the speed variation profile from the mass-start race as introduced into the simulation, a set of simulation experiments were run, including: varying the number of cyclists; varying the duration of a single near-threshold output event; and varying the course elevation. The results consistently show sorting of pelotons into smaller groups whose mean fitness corresponds with relative group position, i.e. fitter groups are closer to the front. Sorting of pelotons into fitness-related groups provides insight into the mechanics of similar group divisions within biological collectives in which members present heterogeneous physiological fitness capacities.

© 2014 Elsevier Inc. All rights reserved.

1. Introduction

Pelotons are groups of cyclists coupled by power-output reduction (energy-savings) benefits of drafting. Pelotons may include as many as 200 cyclists, as observed in mass-start bicycle races such as the Tour de France [1].

There is extensive academic literature related to bicycle racing as a sport. This literature can be grouped into three broad categories: bicycle engineering and design, racing strategy, cyclists' physiology and training methods. See [2] for several recent examples. Research involving cycling as a sport, however, generally does not involve quantitative or substantive qualitative analysis of the collective dynamics of pelotons.

The analysis of cyclists' collective dynamics may be traced to the research of Kyle [3] in 1979, which examined the benefits of drafting, thus setting the theoretical basis for the coupled behavior of cyclists. Research involving drafting was subsequently developed empirically and theoretically [e.g. 4–6]. However, it appears the coupling dynamics of drafting were not extended theoretically to more general group dynamics until Olds' analysis of the factors affecting the success or failure of

* Corresponding author.

E-mail addresses: htrenchard@shaw.ca (H. Trenchard), E.Martins-Ratamero@warwick.ac.uk (E. Ratamero), ashy@uvic.ca (A. Richardson), matjaz.perc@uni-mb.si (M. Perc).

separated groups of competitive cyclists [6]. Consequently, Olds' analysis arguably represents the first published analysis of self-organized collective peloton behavior.

We see therefore that along with the growth of complex systems science, research into the collective dynamics of pelotons is in its infancy. Only recently have the collective dynamics of pelotons been recognized to fall within the domain of complex systems science, and thus recognized to exhibit properties that are applicable among a variety of biological and non-biological systems [7–16].

Two main branches of the collective behavior of pelotons are developing. The first branch relates to self-organized pattern formations in non-competitive environments, primarily in the context of their urban traffic patterns [17,18] (“non-competitive pelotons”).

The second major branch relates to self-organized dynamics of pelotons in a competitive environment (“competitive pelotons”), which in turn can be divided into two sub-categories. The first of these sub-categories is an economic, resource based, or game theoretical analysis of cyclists' cooperation and defection strategies, largely derived from the energy savings benefits of drafting [9,10,19,20] (“game theoretical peloton applications”). Somewhat less clearly delineated, but appropriately falling within the sub-category of game theoretical peloton applications is a study of the exogenous influence of league organizational structure on the competitive dynamics of bicycle racing [21].

The second sub-category of research into competitive pelotons relates to physical self-organized formations that emerge from the collective interactions of cyclists in a competitive environment [7,11–16,21–23]. The intersection between principles underlying the collective dynamics of pelotons and energy savings mechanisms of biological systems has been proposed [11], based largely on research identifying energy savings mechanisms in a variety of collectives including bird flocks in flight [24], sperm formations [25,26], huddling penguins [27], fish schools [28], ducklings on-water formations [29], and drafting among dolphins [30]. The intersection of competitive peloton dynamics and other biological collectives may be extended (but not limited to) to include positional analysis of fish based on aerobic capacities [31], similarities of peloton formations and collective formations among coot birds [32], as well as contrary evidence of the metabolic benefits of caterpillar aggregations [33].

2. Mathematical model

A cyclist's power requirement to overcome wind resistance is proportional to the cube of his or her velocity [34]. Power requirements when drafting, for a single rider are reduced by approximately 18% at 32 km/h (~20 mi/h), 27% at 40 km/h (~25 mi/h); and by as much as 39% at 40 km/h among a group of eight riders [4]. For two riders, drafting benefit is negligible at speeds below 16 km/h (10 mi/h) [35].

When cycling in groups, cyclists' sustainable speeds increase according to drafting benefits, leaving the sustainable power output unchanged for drafting cyclists. For example, based on power output ranges reported in [36] a drafting cyclist with a hypothetical maximum power output of 349 W can sustain the speed of a stronger rider up to ~52 km/h (~32 mi/h) on a flat, windless course, and yet may sustain only approximately 41 km/h under the same conditions, without drafting benefit.¹

Cyclists' maximal sustainable power outputs (“MSO”) depend upon individual physiological capacities, and vary as a function of the duration of the output [38]. A cyclist's MSO may be determined if her maximal oxygen uptake parameter (VO_{2max}) is known [39]. For the cyclists whose data is applied in this paper, VO_{2max} values are unknown. However, reasonable estimates of these cyclists MSOs were derived from publicly available sprint times and corresponding power outputs, as discussed further.

Pelotons frequently divide into smaller groups, as in Fig. 1. Generally, pelotons divide when the power-output reduction benefit of drafting is no longer sufficient to compensate for the differences in strength between weaker and stronger cyclists. For example, as course inclines increase (i.e. hills), drafting benefit diminishes due to reduced speed, while power-output remains high; in such conditions pelotons tend to divide frequently and into numerous groups, as in Fig. 1 (lower left). For flatter terrain pelotons tend to divide less frequently, indicating that drafting benefits are sufficient for weaker cyclists to sustain the speeds of stronger cyclists, as in Fig. 1 (lower right and upper left).

However, even at high speed on relatively flat courses, pelotons may also undergo division due to fatigue induced at sustained high speed or due to coupling instabilities, or a combination of these factors. Coupling due to drafting is inherently unstable as cyclists continuously adjust their positions, periodically exposing following riders to the wind. This necessitates a rapid response from following cyclists in order to maintain optimal drafting position. Following cyclists are particularly susceptible to increased wind exposure on circuitous or narrow courses; cross-winds, or high density configurations when riders compete for optimal drafting positions. High density situations are particularly unstable due to the high probability of crashes at a critical density threshold.

To demonstrate the mechanics of peloton divisions, we further develop the “peloton-convergence-ratio” (PCR) expression [14]:

$$PCR = \frac{P_{front} - (P_{front} * \frac{D}{100})}{MSO} \quad (1)$$

¹ Approximated by reference to drafting equations in [3,6], and speed to power conversions in [37].

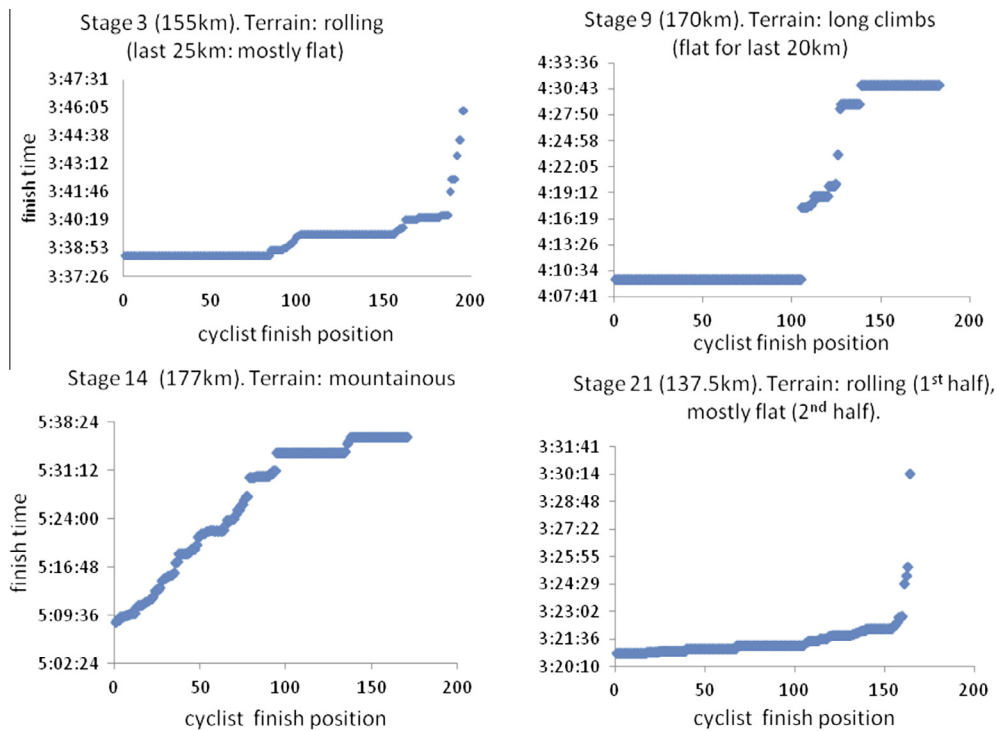


Fig. 1. Results of four stages of the 2014 Tour de France [1]. Flat or rolling courses with flat finishes tend to produce a relatively small number of groups of riders finishing together; such groups tend to finish within narrow time intervals (upper left, and lower right). Mountainous races with uphill finishes tend to produce more numerous, smaller groups (lower left); courses with long climbs and relatively long flat finishes tend to produce larger, less numerous groups than mountainous races, but which finish within wider time intervals than flat races (upper right).

This refers to the situation of two coupled riders: the non-drafting front-rider sets the pace; the follower enjoys the drafting benefit and maintains the same speed, at a lower power output. Two-cyclist coupling is a simple principle that readily generalizes to more complex, many-rider interactions. Moreover, all drafting cyclists are coupled to both the rider immediately ahead who provides the drafting benefit for the follower, and also to a single non-drafting cyclist at the front of the peloton, or a relatively small number of non-drafting cyclists at the front who set the pace. Here we refer to a “front-rider” as a non-drafting cyclist who sets the pace; a “leader” is a cyclist immediately in front of a drafting rider, but who herself may be drafting behind other riders.

In (1), “ P_{front} ” is the power output of the front-rider as she sets the pace within the coupled system. “ D ” expresses the follower’s energy savings due to drafting, as a fraction (percentage) of the front-rider’s power output. Thus, the follower’s required power output is ($P_{front} * (D/100)$), assuming approximately equal factors affecting required power output for all riders, aside from drafting.² Finally, MSO is the maximal sustainable power output for the follower: should P_{front} exceed MSO , the follower will be unable to sustain the leader’s (and front-rider’s) speed and must decelerate to a speed less than or equal to that speed representative of the limitation of MSO .

A drafting cyclist may operate at or below MSO . If she is at MSO while drafting but conditions change (e.g., the rider falls too far behind or too far to the side of the optimal drafting position, with respect to the leader), then the follower must decelerate. If she is below MSO while drafting but temporarily falls outside drafting range, she can increase power output to maintain the pace of the leader as long as she does not exceed MSO .

PCR can also be expressed in the form:

$$PCR = \frac{P_{front} - [P_{front} * (1 - d)]}{MSO}, \quad (2)$$

where the term $1 - d$ is written instead of $D/100$; and where d is the drafting coefficient:

$$d = 0.62 - 0.0104d_w + 0.452d_w^2. \quad (3)$$

² The following parameters are used to determine cyclists’ power output (in W): frontal area of cyclist = 0.639 m²; drag coefficient = 0.5; coefficient for power transmission losses and losses due to tire slippage = 0.015; air density = 1.226 kg m⁻³; coefficient of rolling resistance 0.004; mass of rider and bicycle = 75 kg; coefficient for velocity-dependent dynamic rolling resistance (CrV), approximated 0.1; coefficient for the dynamic rolling resistance, normalized to road inclination CrV * cos(β); rolling friction plus slope pulling force (Frg) = 9.8 * Wkg * ((crr * cos gradient) + (sin gradient)); gradients variable.

Eq. (3) is from Olds [6], who referred to this coefficient as “ CF_{draft} ” (which he derived from data presented in [3]).

Rearranging (2) the front-rider’s power output (“ P_{front} ”) is:

$$P_{front} = \frac{MSO * PCR}{d}. \tag{4}$$

To find the threshold representing the greatest speed a cyclist is able to maintain, we convert “ P_{front} ” to velocity (V_{front}) using power output relationships and parameters as in [40; Appendix A] and [41]. A (weaker) follower must decelerate to a speed less than or equal to the speed corresponding to $PCR = 1$, so we want to know her power output corresponding to her physiological threshold, MSO , while drafting (i.e., $PCR = 1$):

$$P_{threshold} = \frac{MSO}{d}. \tag{5}$$

This is identical to (4) with the assumption $PCR = 1$. Then, “ $P_{threshold}$ ” represents power output reduction due to drafting when $PCR = 1$.

Thus the expression $P_{front} - P_{threshold}$ allows us to obtain the follower’s speed that corresponds to her MSO . First converting “ $P_{threshold}$ ” to an equivalent speed (“ $V_{threshold}$ ”) using the same power-speed relationships as before [40, Appendix A], we then take the difference of the two values (6), obtaining the difference between the speed set by the (stronger) front-rider and the (slower) speed which is the maximal speed available to the (weaker) rider:

$$V_{reduction} = V_{front} - V_{threshold}. \tag{6}$$

“ $V_{reduction}$ ” thus represents the deceleration magnitude for the following rider, in the event her required output to maintain the speed of a front-rider corresponds to an output that exceeds her MSO ($PCR > 1$).

When cyclists decelerate to keep their output at or below MSO , they usually slow to an output below, but not exactly at the threshold (on an individually varying basis). Therefore it is reasonable to add a small random magnitude of deceleration (6), as follows:

$$V_{reduction} = V(P_{front}) - V(P_{threshold}) + \Delta V. \tag{7}$$

Eq. (7) summarizes our model for determining a speed update to apply to the weaker (following) rider, given the circumstance $PCR > 1$ (that is, the follower is no longer able to keep pace with the front-rider). In (7), “ $V(P)$ ” term is a velocity “ V ” expressed as a function of a power “ P ”, and Δ is the aforementioned small (positive) random (individual) deceleration quantity.

We incorporate (7) into the computer peloton dynamics model by Ratamero [42]. In addition, some adjustments to Ratamero’s cohesion and separation rules are given. Finally, we also adjust Ratamero’s drafting parameter, to account for increased drafting benefit for multiple drafting cyclists [42].

3. Simulation design

In [14] positional profiles of 14 female cyclists in a 30 lap (333 m/lap) velodrome race (the “Points Race”) was shown, as in Fig. 2.

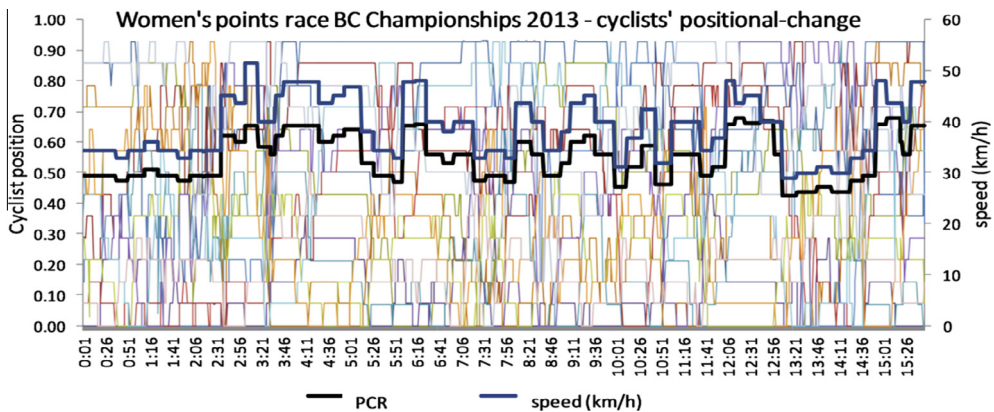


Fig. 2. Women’s 30-lap Points Race: positional-profiles. The heavy blue curve is speed; the heavy black curve is the Peloton Convergence Ratio (PCR). Periods of high trajectory intersection (e.g. between time $\sim 0:01$ and $\sim 2:31$) indicate frequent and comparatively long-distance positional change among cyclists corresponding to low speed and PCR , while periods shown by parallel lines (e.g. between time $\sim 4:00$ and $\sim 5:01$) indicate single-file formation corresponding to comparatively high speed and PCR . These distinct periods delineate phases of peloton behavior. (For interpretation of the references to color in this figure legend, the reader is referred to the web version of this article.)

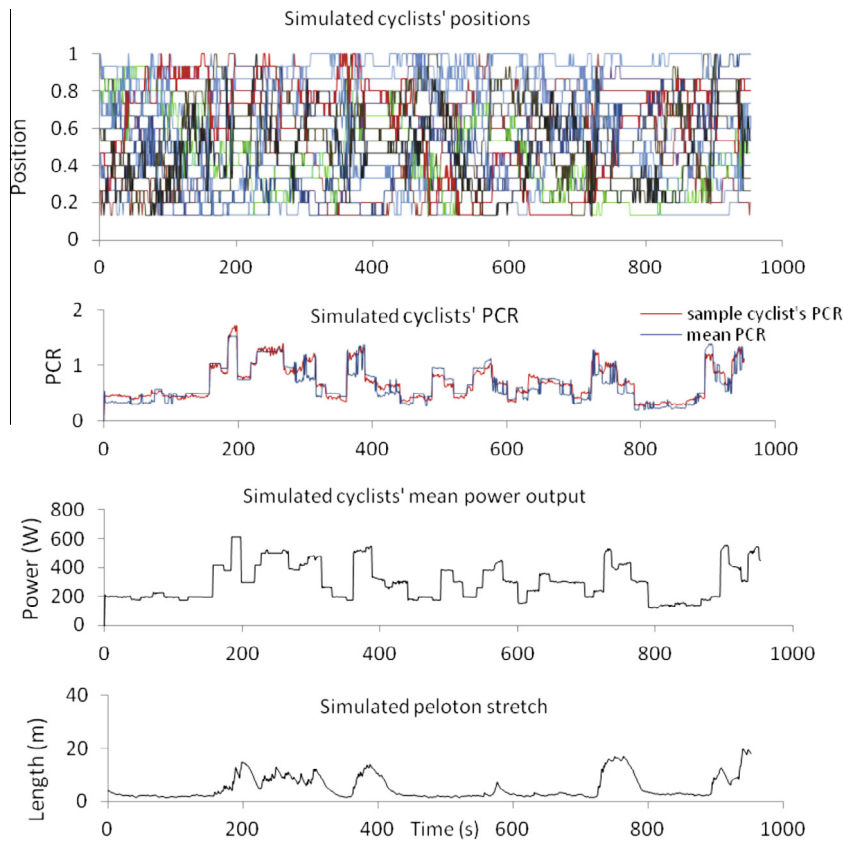


Fig. 3. Typical simulated race profile for 14 cyclists, using *MSO* and speed data derived from the Points Race data. In the upper graph, the zero (front-most) position was not computed. Peloton stretching is represented by parallel line patterns which indicate cyclists travel in single-file. The mean power output (among all cyclists) is shown in the third plot, while a simulated peloton stretch parameter is shown in the lower image (plotted against time, in seconds).

For the purpose of the model introduced here, the speed data from the Points Race are analyzed to derive parameters for the simulation experiments.

Accordingly, 200 m sprint times of 11 of the 14 cyclists in the Points Race, achieved during sprint trials prior to the Points Race, were used to determine equivalent power outputs (in W) required to sustain their 200 m average speeds. The average power output of the 11 cyclists (397 W) was used to represent the values of three cyclists in the Points Race who did not participate in the sprint trials.

These power outputs were then multiplied by a coefficient of 0.82. This coefficient 0.82 is the fraction (399 W/485 W) where 399 W is power at 48 km/h and 485 is power at 51.4 km/h. The former (48 km/h) is the maximum speed sustained for a duration greater than 30 s (39 s) representing the maximal aerobic power threshold sustainable for a duration of between 30 s and ~5 min [38]. The latter (51.4 km/h) is the absolute maximum speed attained during the Points Race (15 min 53 s in duration).

These power outputs were then applied as *MSO* data for all simulation experiments involving 14 simulated cyclists. The power outputs are, in descending order:

479 458 435 412 402 400 397 397 397 393 372 356 351 305

For all simulation experiments involving greater than 14 cyclists, random power output values in the range 305–479 W were used (the lower and upper thresholds represent the two extreme *MSOs* from the Points Race data). Thus, small variations in mean *MSO* are observed, between experiments.

MSO data accuracy is further limited because there are multiple variables determining power output. For example, the course surface roughness, the mass and frontal surface area of the cyclist, and the absence or presence of wind (even at low speeds) will affect power output as a function of speed. Here, these parameters were not precisely determined, although it is possible to assume reasonable estimates for their values (see footnote 2). For the races, minimal wind was observed. Further, *MSO* constantly changes for each cyclist as fatigue temporarily reduces *MSO* [43]. Consequently, it was not practical

Table 1

Outline of the simulation protocol. For each run, the precise speed profile derived from the Points Race data (Fig. 2) was coded into the algorithm as a constant parameter.

Variable		Runs
14 Cyclists	3% Hill	10
	One 4% hill	“
	Flat	“
25 Cyclists	3% Hill	“
	One 4% hill	“
	Flat	“
50 Cyclists	3% Hill	“
	One 4% hill	“
	Flat	“
100 Cyclists	3% Hill	“
	One 4% hill	“
	Flat	“

to obtain accurate empirical measures of *MSO* power outputs; in this light the values discussed represent reasonable estimates.

Introducing *MSO* and speed data as observed in the Points Race, and running a series of tests to fine-tune cohesion/separation parameters established in [14], we obtain typical parameter profiles, as in Fig. 3.

The cohesion and separation parameters (“CS parameters”) adjust the range in which the “attractive force” of centroid (mean *x*–*y* coordinate) positioning applies [42]. CS parameter values are small relative to the actual forward speed parameter values [42] and for this model the CS parameter values are also small relative to deceleration parameter values. The CS parameters were balanced heuristically against the deceleration parameter values, seeking to obtain the profile shown in Fig. 2.

Keeping constant the speed profile as observed during the Points Race, simulation tests were run as shown in Table 1. This sequence of tests included increasing the size of the simulated peloton from 14 riders to 25, 50, and 100 riders, with no change in hill gradient. We also varied the durations at which cyclists proceeded at specific power outputs by varying the hill gradient in two circumstances: (1) for the entire simulation (“3% hill”) (simulation time equivalent to 15:53 min); (2) for a single period of 19 s when cyclists traveled at 39.9 km/h, during which the gradient was increased from 0% to 4% (“One 4% hill”). Immediately prior to the One 4% hill period, cyclists traveled at 51.4 km/h for 14 s. By increasing the gradient to 4% for a further 19 s immediately following the absolute maximum speed of 51.4 km/h, simulated cyclists were forced to sustain nearly the same absolute maximum power output for a total of 33 s. Thus the One 4% hill was incorporated to test the effect on peloton dynamics of an extended period of sustained near maximal power output. In all three sets of experimental simulations, speeds were not varied from the original speed profile obtained from the Points Race. For each combination we observed whether peloton division and/or sorting occurred.

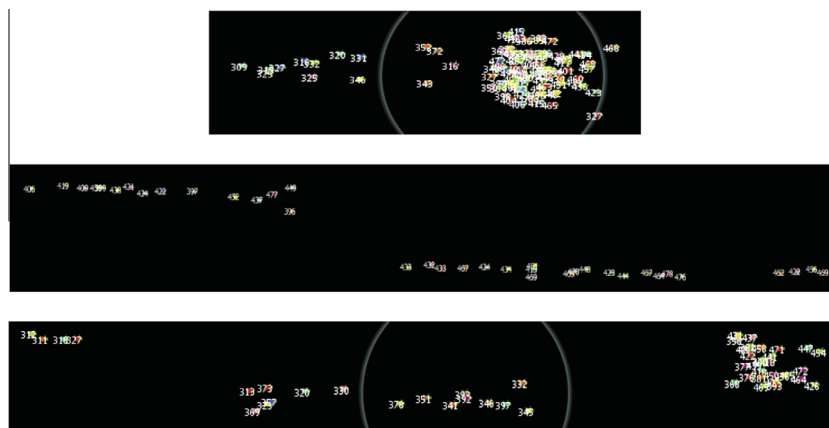


Fig. 4. Three typical end states from simulated bicycle peloton dynamics. The upper image shows 100 cyclists in a simulation with “flat” terrain; low peloton stretch and low group division are observed (individual *MSO* values are shown). The middle image shows a segment of 100 cyclists traveling on “3% hill” terrain: high peloton stretching and division into three main groups is observed. The lower image shows 50 cyclists with “one 4% hill” terrain slope variation: peloton stretching and division are observed: one high density group is seen at the front (far right) as stretched groups follow behind.

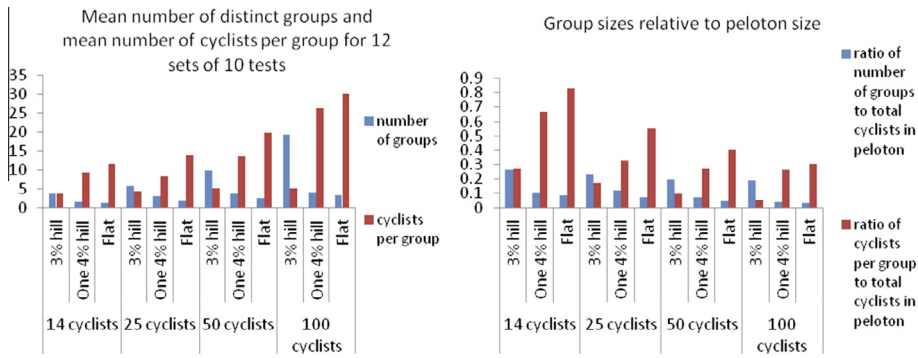


Fig. 5. (panel a) Mean number of distinct groups and number of cyclists per group, per test. Generally, simulated pelotons tended to divide most frequently when high power outputs were sustained (“3% hill”), as expected. Pelotons tended to split less frequently on flat courses and when a single extended high output period was introduced (“One 4% hill”). (panel b) Ratios of group size to total peloton size indicate that smaller pelotons on flat courses produce greatest cohesion; introducing a single extended high output period produced somewhat dropping cohesion (increasing division), while constant high output (“3% hill”) produced high peloton division.

4. Results and discussion

There is remarkable agreement between the actual Points Race positional profile (Fig. 2), and the simulated positional profile, according to the upper image of Fig. 3. These profile similarities validate model parameters. Realistic collective positioning according to cyclists’ inherent abilities (*MSO*), speeds, and output ratios (*PCR*) emerge, as in Fig. 4.

There is also general agreement in the nature of the peloton divisions in comparing the Tour de France results (Fig. 1) with the simulation experiment results. Where power output is sustained near threshold for all riders (e.g., for “3% hill” gradient, as in Fig. 4, middle image) pelotons tended to divide into smaller groups, as also shown in Fig. 1 (lower left: “mountain” finish). Overall, flat courses produce small numbers of groups, supporting the results indicated in Fig. 1 (upper left and lower right images), as in Fig. 5 (panel a).

Simulation results support the intuitive prediction that groups positioned behind the leading group tend to contain riders with lower mean *MSO*, corresponding to group order, as in Fig. 6.

This trend is consistent across experimental groups. Cyclists’ finishing positions in Fig. 1 can thus be compared with simulation results and, particularly for mountainous terrain (lower left), extrapolated to correspond with relative cyclist fitness.

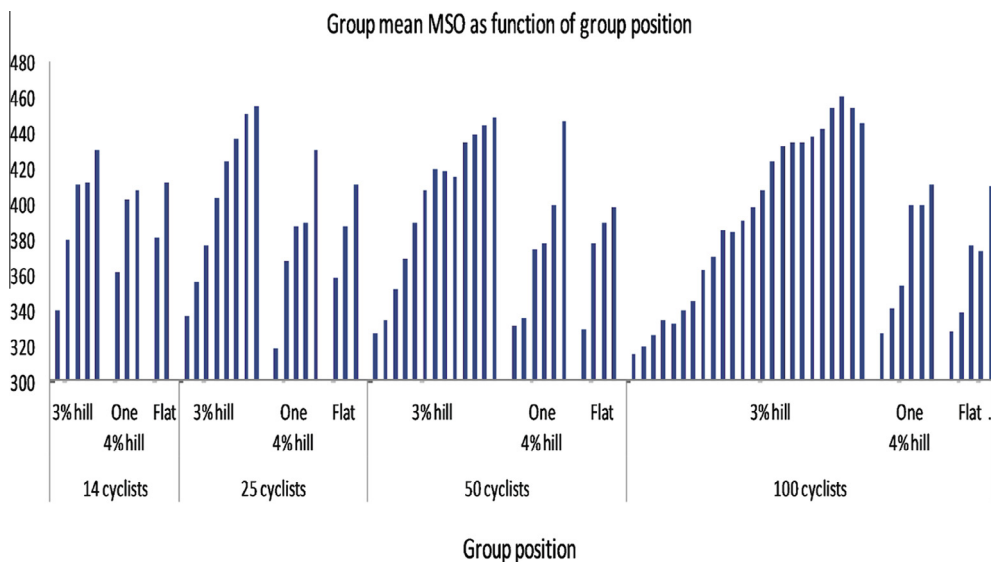


Fig. 6. Mean group *MSO* descends in correspondence to group position. Groups farthest from the front (to the left) exhibit lower mean *MSO*. This demonstrates the group sorting effect where increasing speeds drive cyclists close to *MSO* for sustained periods. Hence weaker cyclists are separated from stronger cyclists, but each of whom form smaller groups containing cyclists with heterogeneous fitness capacities, but descending mean *MSO* in correspondence to relative sub-dominant group position.

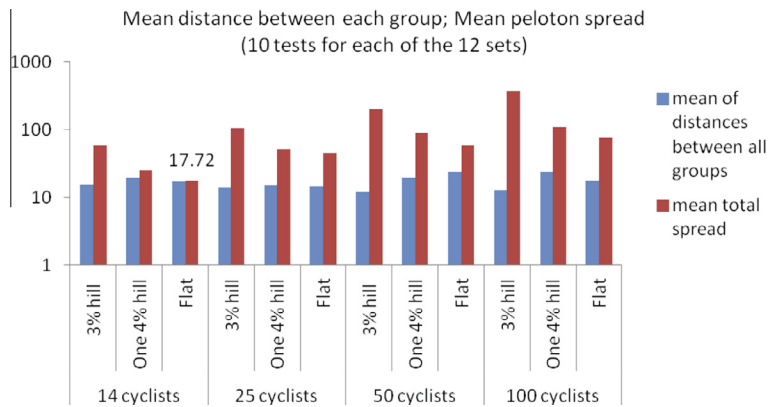


Fig. 7. Log plot of mean distance between all groups for each set of tests and total group spread (distance between first and last simulated cyclists). Spread for 14 cyclists on the flat course is shown in comparison with the actual Points Race spread (~63 m). Log plotting is used to compress scale. Despite comparatively constant distance between groups in all cases, total group spread is clearly greater when there is constant high power output over the course of the experiment, as for cases of 3% hill, as well as for a single extended high output event as in One 4% hill. This is expected since groups of cyclists with lower mean MSOs will gradually lose ground on fitter groups.

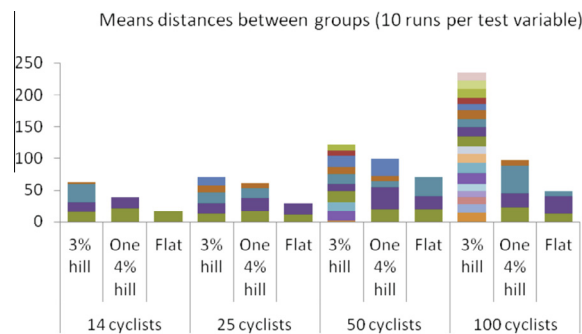


Fig. 8. Stacked distances between each group, as indicated by colored blocks. Since blocks represent space between groups, the number of groups equals $n + 1$, where n is the number of colored blocks (this does not include single cyclists between groups, which were not counted). Similarly to Fig. 6, histogram demonstrates that overall total spread between discreet groups increases as groups with lower mean MSO lose ground to faster groups when output is sustained, while groups divide less readily for a single extended event (4% hill), but nonetheless more so than for experiments on a flat course.

The model is less persuasive in terms of its peloton stretch. In the Points Race, peloton stretch at the finish was observed to be approximately 63 m, compared to a mean stretch of approximately 18 m over 10 tests, as in Fig. 7.

This difference may be partly explained by cyclists “giving up” at the end of the race, decelerating to a speed corresponding to an output well below *MSO*, thereby stretching the peloton more than if the race had continued such that cyclists maintained power output at *MSO* (as was the case for the simulation). Such resignation among riders at the finish of a race is common when only a few of the top positions are contested in earnest during a final all-out sprint, resulting in anomalous stretching at the end of the race that would not occur during vast majority of the race as all riders seek to maintain contact with the peloton. Additionally, this difference in simulation versus actual stretch data may be further explained by accumulated fatigue at the finish that was not captured in the simulation.

Conversely, simulation parameters may also be responsible for the truncated simulation end-state peloton stretch. This suggests that the balance between CS parameters, speed and deceleration parameters could be further fine-tuned to match the real world data. Moreover, the balance among the parameters, while shown to be set with reasonable accuracy for the 14 cyclists in the Points Race, may become less realistic for group sizes substantially different than 14.

The truncated simulation stretch, as shown in Fig. 8, suggests the final distances between simulated groups may not precisely reflect real-world separations between groups.

However, this does not substantially undermine the integrity of the model in demonstrating the group sorting dynamic, which is robust across a variety of experimental parameters. Moreover, the simulation stretch (lower image, Fig. 3) which shows short term high stretch, followed by increased peloton density, reflects with reasonable accuracy the oscillation dynamics of the actual Points Race, in which the peloton remained generally cohesive for the whole race.

5. Conclusions

Overall, the agreement between simulated and actual race profiles supports the viability of the model as evidence of actual peloton dynamics. The model is reasonably accurate in terms of its deceleration parameter and the resulting oscillation between stretching (decreased density) (as speeds temporarily reach speed above that corresponding to *MSO*), and increased density (as speeds relax when cyclists in a given group are generally below their individual *MSO*). The model well supports the supposition that, at high relative outputs, sub-groups form that are composed of cyclists with lower mean *MSO*, in correspondence with sub-dominant group position.

One weakness of the model is that simulated bicycle peloton dynamics may not be accurate when the average speed is well below that corresponding to *MSO*, yet the peloton is in a high density state. For example, an observed convective phase is thought to occur within such a range of parameters, whereby cyclists freely pass others in general movement toward the front around the peloton periphery [12,14,42]. The present model has not been tested for the emergence of this phase dynamic, although a model of this phase does exist [42]. Elements of a backwards convection, as discussed in [14] do appear to correspond with the deceleration phase, however, measurements of long-term equilibrium backwards-convective states were not attempted here. Further experiments may be run to test for the presence of this dynamic.

Empirical data that includes VO_{2max} values for cyclists may be compared with the simulation results here. Similar measurements of aerobic capacity, speed, and coupling parameters may be sought for other biological collectives. We predict that by driving groups to reach power outputs near the maximally sustainable level, group sorting will occur in a manner similar to that observed for bicycle pelotons. Empirical studies for other such biological collectives will be needed to test this prediction, as well as to inform the selection of model parameters in order to test whether the model produces the proposed dynamics.

Acknowledgments

M.P. is funded by the Slovenian Research Agency (Program P5-0027) and the Deanship of Scientific Research (DSR), King Abdulaziz University, under Grant No. (76-130-35-HiCi).

Appendix A

Power:

$$P = C_m V \left(C_d A \frac{p}{2} (V + W)^2 + F_{rg} + V C_{rvn} \right). \quad (8)$$

Speed:

In order to solve this Power equation for velocity V , we write it in the implicit form

$$V^3 + 2V^2 \left(W + \frac{C_{rvn}}{C_d A_p} \right) + V \left(W^2 + \frac{2F_{rg}}{C_d A_p} \right) - \frac{2p}{C_m C_d A_p} = 0, \quad (9)$$

so we can use Cardano's formulae to obtain the solutions:

If $a^2 + b^3 \geq 0$:

$$V = \sqrt[3]{a + \sqrt{a^2 + b^3}} + \sqrt[3]{a - \sqrt{a^2 + b^3}} - \frac{2}{3} \left(W + \frac{C_{rvn}}{C_d A_p} \right). \quad (10)$$

If $a^2 + b^3 < 0$ (casus irreducibilis; in case of sufficient downhill slope or tailwind speed):

$$V = 2\sqrt{-b} \cos \left(\frac{1}{3} \arccos \frac{a}{\sqrt{-b^3}} \right) - \frac{2}{3} \left(W + \frac{C_{rvn}}{C_d A_p} \right), \quad (11)$$

with

$$a = \frac{W^3 - C_{rvn}^3}{27} - \frac{W \left(5WC_{rvn} + \frac{8C_{rvn}^2}{C_d A_p} - 6F_{rg} \right)}{9C_d A_p} + \frac{2F_{rg} C_{rvn}}{3(C_d A_p)^2} + \frac{p}{C_m C_d A_p}, \quad (12)$$

and

$$b = \frac{2}{9C_d A_p} \left(3F_{rg} - 4WC_{rvn} - W^2 C_d A \frac{p}{2} - \frac{2C_{rvn}}{C_d A_p} \right). \quad (13)$$

P	rider's power
V	velocity of the bicycle
W	wind speed
H_{nm}	height above sea level (influences air density)
T	air temperature, in ° Kelvin (influences air density)
grade	inclination (grade) of road, in percent
β	("beta") inclination angle, = arctan(grade/100)
m_{bike}	mass of the bicycle (influences rolling friction, slope pulling force, and normal force)
m_{rider}	mass of the rider (influences rolling friction, slope pulling force, and the rider's frontal area via body volume)
C_d	air drag coefficient
A	total frontal area (bicycle + rider)
C_r	rolling resistance coefficient
C_{rV}	coefficient for velocity-dependent dynamic rolling resistance, here approximated with 0.1
C_{rVn}	coefficient for the dynamic rolling resistance, normalized to road inclination; $C_{rVn} = C_{rV} \cos(\beta)$
C_m	coefficient for power transmission losses and losses due to tire slippage (the latter can be heard while pedaling powerfully at low speeds)
ρ	("rho") air density
ρ₀	air density on sea level at 0° Celsius (32°F)
p₀	air pressure on sea level at 0° Celsius (32°F)
g	gravitational acceleration
F_{rg}	rolling friction (normalized on inclined plane) plus slope pulling force on inclined plane

References

- [1] <<http://www.letour.com/le-tour/2014>>, accessed August, 20 2014.
- [2] J. of Sci. and Cycling, Book of Abstracts, in: 2nd World Congress of Cycling Science 2014, Leeds (2014).
- [3] C. Kyle, Reduction of wind resistance and power output of racing cyclists and runners travelling in groups, *Ergonomics* 22 (1979) 387–397.
- [4] S. McCole, K. Clancy, J.C. Conte, R. Anderson, J.M. Hagberg, Energy expenditure during bicycling, *J. Appl. Physiol.* 68 (1990) 748–753.
- [5] B. Blocken, T. Defraye, E. Koninckx, J. Careliet, P. Hespel, CFD simulations of the aerodynamic drag of two drafting cyclists, *Comput. Fluids* 71 (2013) 435.
- [6] T. Olds, The mathematics of breaking away and chasing in cycling, *Eur. J. Appl. Physiol.* 77 (1998) 492–497.
- [7] H. Trenchard, G. Mayer-Kress, Self-organized coupling and synchronization in bicycle pelotons during mass-start bicycle racing, in: Book of Abstracts of Intl. Conf. on Control and Synchronization in Dynamical Syst., Leon, Gto, Mx, 2005.
- [8] H. Trenchard, Hysteresis in competitive bicycle pelotons, complex adaptive systems – resilience, robustness and evolvability, in: Papers from AAAI Fall Symposium FS-10-03, 2010, pp. 130–137.
- [9] R. Hoeningman, E. Bradley, A. Lim, Cooperation in bike racing—when to work together and when to go it alone, *Complexity* 17 (2) (2011) 39–44.
- [10] H. Trenchard, Information flow and the distinction between self-organized and top-down dynamics in bicycle pelotons, in: Papers from AAAI Fall Symposium Complex Adaptive Systems – Energy, Information, and Intelligence, 2011, pp. 144–152.
- [11] H. Trenchard, Energy savings in bicycle pelotons, a general evolutionary mechanism and a framework for group formation in Eusocial evolution, in: H. Sayama, A. Mina, D. Braha, Y. Bar-Yam (Eds.), Proc. of the Eighth Intl. Conf. on Complex Sys., New England Complex Systems Institute Book Series, Unifying Themes in Complex Systems, vol VIII, 2011, pp. 736–750.
- [12] H. Trenchard, The complex dynamics of bicycle pelotons, <<http://arxiv.org/ftp/arxiv/papers/1206/1206.0816.pdf>>, 2012.
- [13] H. Trenchard, Peloton phase oscillations, *Chaos Solitons Fractals* 56 (2013) 194.
- [14] H. Trenchard, A. Richardson, E. Ratamero, M. Perc, Collective behavior and the identification of phases in bicycle pelotons, *Phys. A* 405 (2014) 92–103.
- [15] N. Balague, C. Torrents, R. Hristovski, K. Davids, D. Araujo, Overview of complex systems in sport, *J. Syst. Sci. Complex* 1 (26) (2013) 4–13.
- [16] A. Hirsch, S. Levy, Biking with particles: junior triathletes' learning about drafting through exploring agent-based models and inventing new tactics, *Technol. Knowledge Learn.* 18 (1–2) (2013) 1–29.
- [17] J. Zhang, W. Mehner, F. Andresen, S. Holl, M. Boltes, A. Schadsneider, A. Seyfried, Comparative analysis of pedestrian, bicycle and car traffic moving in circuits, *Proc. Soc. Behav. Sci.* 104 (2013) 1130.
- [18] S. Zhang, G. Ren, R. Yang, Simulation model of speed-density characteristics for mixed bicycle flow—comparison between cellular automata model and gas dynamics model, *Phys. A* 392 (20) (2013) 5110.
- [19] A. Dilger, H. Geyer, The dynamic of bicycle finals: a theoretical and empirical analysis of slipstreaming, *Econ. Anal. Policy* 39 (3) (2009) 429–442.
- [20] J. Cunningham, Can game theory explain bike racing? *Cycle Sci.* 37–38 <<http://info.law.indiana.edu/faculty-publications/cole-game-theory-biking.pdf>>, accessed October 15, 2014.
- [21] L. Rebeggiani, D. Tondani, Organizational forms in professional cycling: an examination of the efficiency of the UCI pro tour, *Int. J. Sport Finance* 3 (2008) 19–41.
- [22] B. Ofoghi, J. Zeleznikow, D. Dwyer, C. Macmahon, Modelling and analysing track cycling Omnium performances using statistical and machine learning techniques, *J. Sports Sci.* 31 (9) (2013) 954–962.
- [23] D. Dwyer, B. Ofoghi, E. Hunstman, D. Rossitto, C. Mcmahon, J. Zeleznikow, The elimination race in track cycling: patterns and predictors of performance, *J. Sci. Cycling* 2 (2) (2013) 6–12.
- [24] H. Weimerskirch, J. Martin, Y. Clerquin, P. Alexandre, S. Jiraskova, Energy saving in flight formation, *Nature* 413 (6857) (2001) 697–698.
- [25] H. Moore, K. Dvorakova, N. Jenkins, W. Breed, Exceptional sperm cooperation in the wood mouse, *Nature* 418 (2002) 174–177.
- [26] Y. Yang, J. Elgeti, G. Compber, Cooperation of sperm in two dimensions: synchronization, attraction and aggregation through hydrodynamic interactions, *Phys. Rev. E* 78 (2008) 061903–061912.
- [27] C. Gilbert, S. Blanc, L. Le Maho, A. Ancel, Energy savings processes in huddling emperor penguins: from experiments to theory, *J. Exp. Biol.* 211 (Pt 1) (2008) 1–8.
- [28] J. Herskin, F. Steffensen, Energy savings in sea bass swimming in a school: measurements of tail beat frequency and oxygen consumption at different swimming speeds, *J. Fish Bio.* 53 (2) (1998) 366–376.
- [29] F. Fish, Kinematics of ducklings swimming in formation: consequences of position, *J. Exp. Zool.* 273 (1995) 1–11.
- [30] D. Weihs, The hydrodynamics of dolphin drafting, *J. Biol.* 38 (8) (2004) 1–23.

- [31] S. Killen, S. Marras, J. Steffensen, D. McKenzie, Aerobic capacity influences the spatial positions of individuals within fish schools, *Proc R. Soc B: Biol. Sci.* 279 (1727) (2012) 357–364.
- [32] H. Trenchard, American coot collective on-water dynamics, non-linear dynamics, *Psychol. Life Sci.* 17 (2) (2013) 183–203.
- [33] R. Schoombie, L. Boardman, B. Groenewald, D. Glazier, C. van Daalen, S. Clusella-Trullas, J. Terblanche, High metabolic and water-loss rates in caterpillar aggregations: evidence against the resource-conservation hypothesis, *J. Exp. Biol.* 216 (2013) 4321–4325.
- [34] E. Burke, E., High-Tech Cycling, Human Kinetics, Champaign, Illinois, 1996.
- [35] P. Swain, Cycling uphill and downhill, *Sportscience* 2 (1998) 4. www.sportsci.org/jour/9804/dps.html, accessed January 13, 2013.
- [36] S. Padilla, I. Mujika, J. Orbañanos, J. Santisteban, F. Angulo, J.J. Goirierna, Exercise intensity and load during mass-start stage races in professional road cycling, *Med. Sci. Sports Exercise* 33 (5) (2001) 796–802.
- [37] <www.analyticcyclist.com>, accessed August 20, 2014.
- [38] J. Pinot, F. Grappe, The 'Power profile' for determining the physical capacities of a cyclist, *Comput. Methods Biomech. Eng.* 13 (S1) (2010) 103.
- [39] T.S. Olds, K.I. Norton, N.P. Craig, Mathematical model of cycling performance, *J. Appl. Physiol.* 74 (2) (1993) 730–737.
- [40] <<http://kreuzotter.de/english/espeed.htm>>, accessed August 22, 2014.
- [41] <www.flacyclist.com/content/java/rideCalc/dist/RideCalculator_v2.xls>, accessed August 23, 2014.
- [42] E. Martins Ratamero, MOPED: an agent-based model for peloton dynamics in competitive cycling, in: International Congress on Sports Science Research and Technology Support, Vilamoura, icSPORTS, 2013.
- [43] D. Bishop, Fatigue during intermittent sprint exercise, *Proc. Aust. Physiol. Soc.* 43 (2012) 9.